Comparison of OFDM and SC-FDE for VLC Systems with a Nonlinear LED Model

Hao Zhang[1], Jian Sun[1], Wensheng Zhang[1], Zhiquan Bai[1], and Cheng-Xiang Wang[2,3]
[1]Shandong Provincial Key Lab of Wireless Communication Technologies,
School of Information Science and Engineering, Shandong University, Qingdao, Shandong, 266237, China.
[2] National Mobile Communications Research Laboratory,
School of Information Science and Engineering, Southeast University, Nanjing, Jiangsu, 210096, China.
[3] Purple Mountain Laboratories, Nanjing, Jiangsu, 211111, China.
Email: sduzhanghao@126.com
{sunjian, zhangwsh, zqbai}@sdu.edu.cn, chxwang@seu.edu.cn

***Abstract*—Single-carrier frequency domain equalization (SC-FDE) and orthogonal frequency division multiplexing (OFDM) are two attractive technologies for visible light communications (VLC). In this paper, we analyze the two schemes in VLC system with direct current (DC) biasing. We investigate the bit error rate (BER) performance of SC-FDE and OFDM schemes with a memory nonlinear light-emitting diode (LED) model in a simulated indoor scenario. The system performance between both schemes and the impact of LED nonlinear distortion are compared and discussed. We through numerical simulations found that the OFDM scheme exhibits a better BER performance compared to SC-FDE scheme although having a higher peak-to-average power ratio (PAPR).**

***Index Terms*—single-carrier frequency domain equalization (SC-FDE),orthogonal frequency division multiplexing (OFDM), visible light communication (VLC), nonlinear LED model**

I. Introduction

The employment of white LEDs enables both illumination and communications at the same time. High-speed Visible Light Communications (VLC) based on these mass-market white LEDs is referred as a promising new green communication technology because of the numerous advantages, including excellent coverage, worldwide available and unlicensed bandwidth, and zero interference with existing radio systems. Therefore, it is expected to play an important role in the future indoor wireless data networks and the coming (beyond) fifth generation (5G) communication [1], [2].

However, the very limited bandwidth (typical a few MHz) and the inherent nonlinear characteristics of LED are crucial factors that affect the practical efficiency of VLC systems [3], which distort the signal and degrade system performance, especially affect the BER performance. Fortunately, the feasibility of numerous approaches to enhance the bandwidths [4], [5] and the modeling of LED nonlinearity [6-8] for mitigating the distortion has been proposed and some outstanding performance have been achieved. In order to obtaining a better performance and high data rates, various methods are adopted for modulating the optical signals in VLC system. The amplitude modulation such as On-Off Keying (OOK) and Pulse-position modulation (PPM) are predominantly used in VLC for that they are not sensitive to nonlinearity, so they are regularly used to mitigate the impact of the distortion caused by nonlinearity but with the disadvantages of inter symbol interference (ISI) and low data rates [3].

With the problems mentioned previously, paper [9] first proposed the use of orthogonal frequency division multiplexing (OFDM) for VLC system and which has been recently adopted as an effective solution to mitigate the detrimental effect of ISI for VLC systems. However, the VLC systems usually employ intensity modulation and direct detection (IM/DD) technique for its simplicity : a photo detector (PD) at the receiver is employed to detect the signal directly and convert the optical power signal into electrical signals but the signal transmitted with the form of optical power must be a real and positive value [10]. Therefore, the classical complex OFDM signal must be modified and converted into real to be suitable to VLC systems. Thus, several VLC-OFDM schemes such as direct current (DC)- biased optical orthogonal frequency division multiplexing (DCO-ODFM) [11,12] and asymmetrically clipped optical OFDM (ACO-OFDM) [13] have been proposed in order to meet the requirement. However, OFDM systems have an inherent high peak-to-average power ratio (PAPR). Compared with OFDM system, the single-carrier frequency domain equalization (SC-FDE) system has a much smaller PAPR of the transmitted signal [14,15], it is regard as an alternative to OFDM due to the robust to ISI with low complexity and much smaller PAPR. In this paper, we will introduce the implementation of basic OFDM and SC-FDE schemes with DC biasing in VLC systems. Based on a memory nonlinear LED model and the channel impulse response (CIR) of a simulated indoor empty room scenario, we analyze the PAPR theoretically and make a comparison of BER performance between the two schemes. We also analyse the impact of LED nonlinear distortion with numerical simulation results.

The remainder of this paper is organized as follows: Section II is the basic system model, including the OFDM and SC-FDE schemes in VLC system, the numerical LED nonlinear model, channel model and noise model. Section III compares the PAPR and BER performance and analysis of simulation results. Finally, we concluded the paper in Section IV.

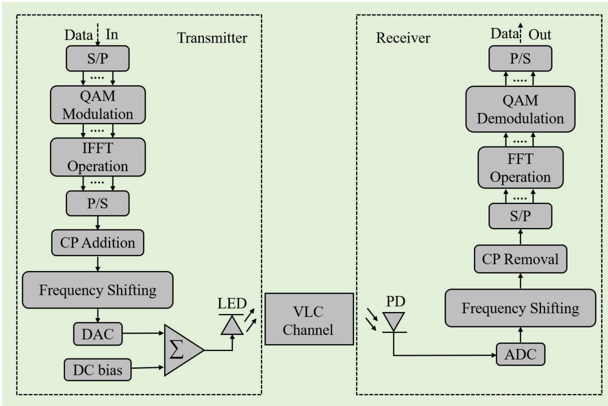

Fig. 1. Block diagram of the SC-FDE system.

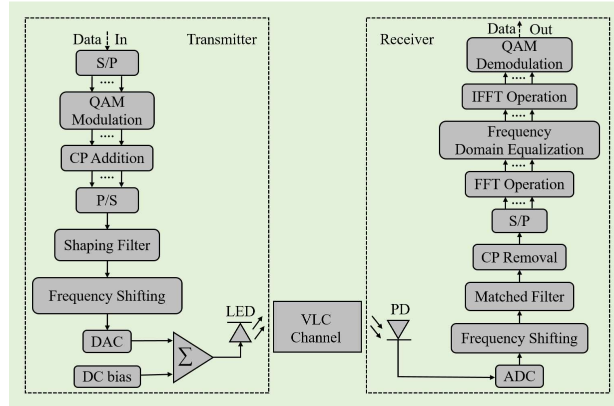

Fig. 2. Block diagram of the SC-FDE system.

II. System model

A. OFDM system

As a modification of OFDM, Fig. 1 shows the block diagram of a typical DCO-OFDM in VLC system. Consistent with classical OFDM system, the binary bit stream is modulated into symbols firstly via multi-level quadrature amplitude modulation (M-QAM)) after transmitted from the source. The generated serial stream of symbols at the modulator output is mapped into parallel streams and all of them is transmitted on a separate subcarrier.

IFFT operation of OFDM system can quickly and efficiently apply the discrete Fourier transform function to generate an orthogonal carrier for transmission, it modulates and multiplexes the subcarriers, the time domain OFDM signal can be generated as expressed mathematically in (1) by taking the IFFT of $X(k)$

$$x(n)=\frac{1}{\sqrt{N}}\sum_{k=-N_c/2,k\neq 0}^{N_c/2-1}X(k)\exp\left\{\frac{j2\pi nk}{N}\right\}, \tag{1}$$

where N is the number of FFT point, $x(n)$ is the n^{th} time domain sample and $n=-T_gN\ldots,N-1$, T_g is the percentage of cyclic prefix (CP) over the block, N_c is the number of effective symbols in each data block, $X(k)$ means the k^{th} frequency domain sample.

But as aforementioned, any complex values must be avoided in VLC-OFDM schemes. To get a real output signal required by IM/DD system, there are two ways of implementation for it generally. One is the application of Hermitian symmetry on the input of the IFFT operation, the other one is to directly employ frequency shift after the IFFT operation. The later way to ensure a real-valued OFDM baseband signal is used in this paper and which is given as

$$\widetilde{x}(n)=\mathrm{Re}\left\{x(n)e^{j\frac{2\pi nBT_S}{2}}\right\}, \tag{2}$$

where B is the bandwidth, T_s is the sampling period.

Usually, after generating the OFDM symbol, we need to make a serial-to-parallel (S/P) conversion and CP is also added as a guard interval. Then a continuous bipolar real signal $X(t)$ can be obtained through digital-to-analog (D/A) conversion. In addition, a DC bias is added to ensure the most bipolar OFDM signals are converted to a unipolar one. The $x(t)$ is the very signal transmitted by LED at the transmitter

$$x(t)=X(t)+I_{dc}. \tag{3}$$

After channel transmission, OFDM symbols are obtained when the optical signal is captured and converted by a photoelectric detector (PD). The processing of signals at the receiver in a DCO-OFDM system is similar to traditional OFDM.

B. SC-FDE system

Single-carrier frequency domain equalization (SC-FDE) is a technology which uses a single carrier to transmit data while reserving the signal processing method of a multi-carrier system. Fig. 2 shows the block diagram of a basic SC-FDE system.

At the transmitter, the input binary data is sent to the channel in the form of data blocks after modulation and CP insertion, the transmitted SC-FDE signal $x(t)$ in the time domain can be expressed as

$$x(t)=\sum_{k=-N_cT_g}^{N_c-1}X\left(k\%N_c\right)\mathrm{g}\left(tT_s-kT\right), \tag{4}$$

where X is modulated N_c symbols and the symbol $\%$ stands for the remainder operation, T is the symbol period, $\mathrm{g}(.)$ is the impulse response of the shaping filter. The frequency shifting operation of SC-FDE is the same as OFDM.

At the receiver, the FFT and IFFT operations are used to achieve a conversion of received data in the time and frequency domain. Frequency domain equalization is to estimate the frequency response of the channel and then use the equalization coefficient to compensate the influence of the channel.

Provided that the received time domain signal at the receiver is $y(t)$, $v(t)$ is the additive white Gaussian noise and the channel impulse response is $h(t)$, then the received signal can be expressed as

$$y(t)=x(t)\otimes h(t)+v(t), \tag{5}$$

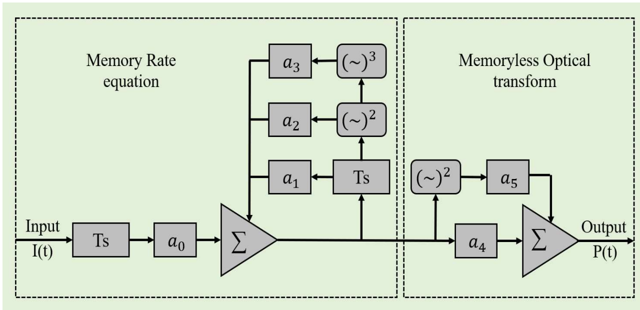

Fig. 3. The block diagram of the memory nonlinear LED model.

where the symbol $\otimes$ denotes convolution.

The frequency domain signal after FFT operation can be expressed as

$$Y(k) = X(k)H(k) + V(k). \tag{6}$$

Zero-forcing (ZF) equalization is considered for signal detection. Assuming the channel frequency response is $H(k)$, the tap coefficients $W(k)$ in the single carrier frequency domain ZF is given by

$$W(k) = \frac{1}{H(k)}, \tag{7}$$

Then the signal after frequency domain equalization can be as

$$\widehat{X}(k) = W(k)Y(k). \tag{8}$$

Finally, the signal after equalized in the time domain can be obtained by performing the IFFT operation.

Comparing Fig. 1 and Fig. 2, it can be found that there are many similarities between OFDM and SC-FDE systems: the data are all transmitted on a block-by-block basis and both of them also use FFT and IFFT operations to implement the conversion between frequency domain and time domain. The main difference between them is the position of FFT and IFFT.

C. LED nonlinear model

Modeling of LED nonlinearity has gained significant attention and some models have been developed. Volterra model is one of the most popular types of these models, which is very convergent to the actual LED and has already been used for LED nonlinearity identification. However, the measurement of the series coefficients of Volterra model [16] is highly complicated.

A numerical nonlinear model based on the physical mechanism of LEDs is proposed in [7] , which can describe LED well but without the drawback of a great complexity like Volterra model. The block diagram of the model is shown in Fig. 3.

Table I lists the specific composition of the coefficients a_0-a_5, which are based on the physical mechanism of LEDs and are used to describe the nonlinear characteristic of LED: a_0-a_3 are used to describe memory rate equation and a_4-a_5 describe the memoryless optical transform. In addition, the input $I(t)$ and output $P(t)$ represents the input current, the output optical power from LED, respectively.

TABLE I
PARAMETERS OF THE MEMORY NONLINEAR LED MOEL

Parameters	Coefficients Composition
Charge of electron(q)	
Active layer thickness(t_w)	
Active layer area(A_w)	$a_0 = T_s/(qt_wA_w)$
Sampling period in simulation(T_s)	$a_1 = 1 - B_rp_0T_s - A_{nr}T_s$
Radiative recombination coefficient(B_r)	$a_2 = -B_rT_s$
Doping concentration(p_0)	$a_3 = -C_{nr}T_s$
SRH recombination coefficient(A_{nr})	$a_4 = \langle E_p \rangle A_wt_wB_rp_0$
Auger recombination coefficient(C_{nr})	$a_5 = \langle E_p \rangle A_wt_wB_r$
Energy of photon (650nm)(E_P)	

D. VLC channel model

In an indoor VLC system, the physical channel model includes both the line of sight (LoS) and the non-line of sight (NLoS) communication components. Compared with the NLoS component, the LoS component is a dominate components in an optical link. In general, we hold that the LED conforms to Lambert emission rule, so the VLC channel can be described as a flat fading channel model [17], and the channel DC gain from the transmitter LED to the PD can be expressed as

$$H = \begin{cases} \frac{(m+1)A}{2\pi D_{tr}^2}\cos^{\mathrm{m}}(\theta)T_s(\psi)g(\psi)\cos(\psi), & 0 \le \psi \le \Psi_c, \\ 0, & 0 > \Psi_c, \end{cases} \tag{9}$$

where, A is the effective detection area of the PD, θ and ψ represent the angle of irradiance and incidence from the LED to the PD respectively, D_{tr} means the distance between the transmitter (Tx) and receiver (Rx), $T_s(\psi)$ is the gain of an optical filter, Ψ_c is the field-of-view (FOV) of the receiver, $g(\psi)$ is the gain of an optical concentrator,

$$g(\psi) = \begin{cases} \frac{n^2}{\sin^2(FOV)}, & 0 \le \psi \le \mathrm{FOV}, \\ 0, & \psi > \mathrm{FOV}, \end{cases} \tag{10}$$

where n denotes the refractive index, m is the Lambertian order, which is related to the semi angle at half-power of the transmit LED,

$$m = \frac{-\ln 2}{\ln\left(\cos \Phi_{1/2}\right)}. \tag{11}$$

This model is a simple but important model for it gives the coefficients of the LoS path. In fact, there exist several investigations and studies were built on the assumption of ideal additive white Gaussian noise (AWGN) channels.

In order to modeling a more practical VLC channel with considering both the LOS and NLOS components, a channel model based on Monte Carlo Ray Tracing was was proposed [18] and the multipath CIR is given as

$$h(t) = \sum_{i=1}^{N_r} E_{Pi}\delta\left(t - \tau_i\right), \tag{12}$$

where E_{Pi} is the power of the i^{th} ray, τ_i stands for the propagation time of the i^{th} ray, $\delta(t)$ is the Dirac delta function and N_r presents the number of rays received at the detector.

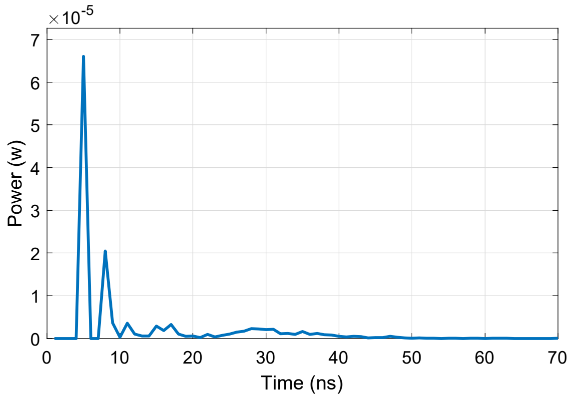

Fig. 4. CIR of the test points C12 and dector location D2.

Fig. 4 shows the multipath CIR of the test points C12 and dector location D2.

E. Noise model

In an optical channel, the signal-to-noise ratio (SNR) can express the quality of communication. The signal component S is given as

$$S = RP_r, \tag{13}$$

where the R means the responsivity of PD, P_r (W/m^2) is the received power which can be defined as (14) when the transmitted optical power is P_t,

$$P_r = H * P_t \tag{14}$$

The noise is composed of shot noise and thermal noise. The shot noise variance is given by [17]

$$\sigma^2_{\text{shot}} = 2qRP_{\text{r}}B + 2qI_{bg}I_2B. \tag{15}$$

The thermal noise is given by

$$\sigma^2_{\text{thermal}} = \frac{8\pi kT_K}{G}\eta AI_2B^2 + \frac{16\pi^2 kT_K\Gamma}{g_m}\eta^2A^2I_3B^3. \tag{16}$$

Thus, the electrical SNR can be defined as

$$SNR(dB) = 10\log_{10}\left(\frac{S^2}{N}\right) = 10\log_{10}\left(\frac{R^2P_r^2}{\sigma^2_{\text{shot}} + \sigma^2_{\text{thermal}}}\right) \tag{17}$$

III. Performance analysis and simulation results

This section will further to verify and discuss the PAPR and BER performance between OFDM and SC-FDE systems with numerical simulation results.

A. Peak to Average Power Ratio (PAPR)

The peak-to-average power ratio (PAPR) is defined as the maximum power of transmitted signal divided by the average power, which is an important indicator to measure the dynamic change of the signal and can be expressed as

$$PAPR(dB) = 10\log_{10}\frac{P_{\text{max}}}{P_{\text{mean}}}. \tag{18}$$

TABLE II
Parameters of OFDM and SC-FDE systems

Parameters	OFDM	SC-FDE
Cyclic Prefix(T_g)	1/8	1/8
Effective symbols(N_c)	62	64
Sampling rate	480MHz	480MHz
Block length	0.6us	0.6us
Oversampling factor	4	4
Bandwidth	∼160MHz	162MHz
Subcarrier bandwidth	1.875MHz	–
Shape filter	–	root raised cosine
Rolloff factor	–	0.35
Symbol rate	–	120MHz
Theoretical PAPR with 16-QAM	23.48dB	9.15dB
Theoretical PAPR with 64-QAM	24.60dB	10.28dB

Specifically, the PAPR of the SC-FDE system can be expressed as the following mathematical expression

$$PAPR_{SC-FDE}(dB) = 10\log_{10}2\beta^2\left(\sum_{l=-N_T}^{N_T}|\mathrm{g}\left(l\alpha T_s\right)|\right)^2, \tag{19}$$

where α is the oversampling factor, N_T is the number of symbols in half length of filter.

For OFDM system, the signal is the sum of the N sub-channel signals, it can be considered that the peak power of the signal is increased by N times, the PAPR of the OFDM system can be expressed as

$$PAPR_{OFDM}(dB) = 10\log_{10}2\beta^2K, \tag{20}$$

where $2\beta^2$ is the peak power when the average power of the modulation symbol is 1 and β equals $\frac{3}{\sqrt{10}}$ and $\frac{7}{\sqrt{42}}$ for 16-QAM, 64-QAM modulation, respectively. In fact, we generally prefer to approximate PAPR as $10\log_{10}K$ for that the probability of PAPR in (20) is extremely small.

Table II lists the parameters and PAPR values of OFDM and SC-FDE systems. It can be seen that the PAPR value of OFDM is significantly greater than SC-FDE, which is caused by the subcarriers superposition of OFDM. In addition, the theoretical calculation results indicate that the effect of the modulation order on PAPR is not very obvious.

B. BER performance simulation and discussion

For both SC-FDE and OFDM system, we set a unified parameter in order to ensure the fairness of the comparison. We adopt a realistic simulation environment: an indoor empty room scenario with dimensions of $6 \times 6 \times 3$m, nine luminaires are fixed on the ceiling with equidistance spacing act as Tx and the arrangement of luminaires and illuminance distribution of this scenario is shown in Fig. 5. The cell phone is equipped with a single PD as Rx and there are seven potential locations for the PD. We consider 100 test points for Rx with equidistant spacing of 0.6 m in x and y directions after selecting the PD location. Then the CIR corresponding to these different positions can be obtained. The numerical results to show the system performance are based on these CIRs.

The inherent nonlinear characteristics of LED are the most crucial factors that affect the practical performance of VLC

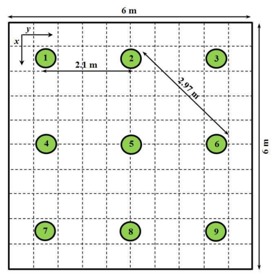

(a) Arrangement of luminaires.

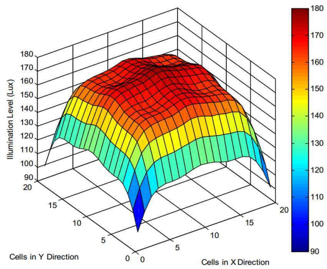

(b) Illuminance distribution.

Fig. 5. The arrangement of luminaires and illuminance distribution of the indoor empty room scenario. Figure reproduced from [18].

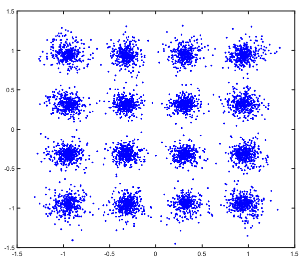

(a)

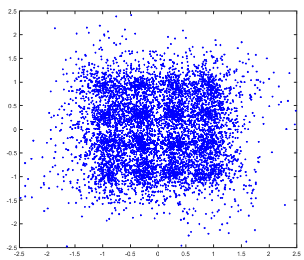

(b)

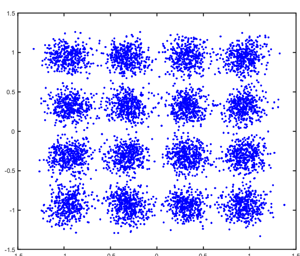

(c)

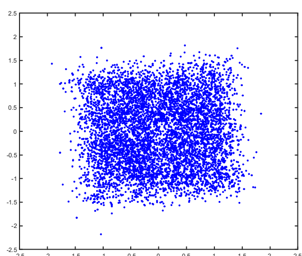

(d)

Fig. 6. Received constellation diagrams of OFDM and SC-FDE with 16-QAM modulation. (a) and (b) OFDM, working in the LED linear and nonlinear region respectively. (c) and (d) SC-FDE, working in the LED linear and nonlinear region respectively.

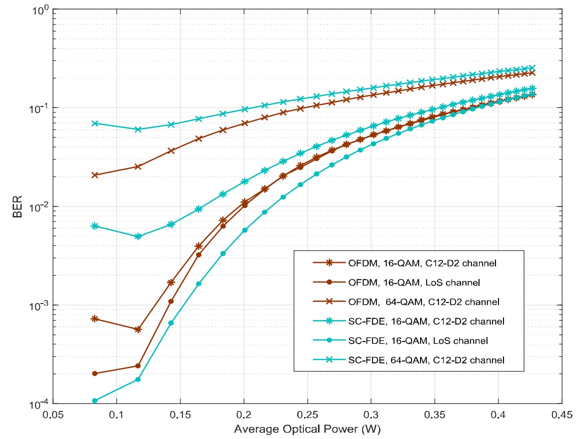

Fig. 7. BER performance of system with nonlinear distortion.

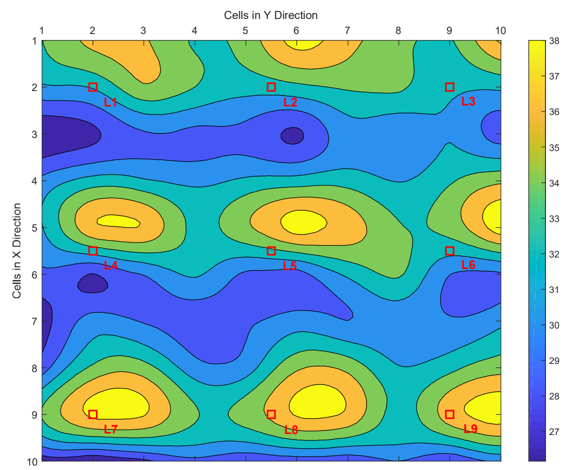

Fig. 8. The SNR distribution of the 100 different test positions in the indoor empty room scenario.

systems. In specifically, both the voltage-current (V-I) relationship and the current-optical power(I-O) relationship in the LED are nonlinear. We add a DC biasing $I_{dc} = 350mA$ to ensure that the LED can meet the illuminance requirements and that the LED works in the operable linear region by adjusting the signal amplitude. While the input signal is too large, the LED will enter the nonlinear region and cause nonlinear distortion in the I-O conversion, which will significantly reduce the performance of the VLC system, especially affecting the BER.

Fig. 6 gives the constellation diagrams of 16-QAM modulation system working among the linear region and the nonlinear region. In addition, to further illustrate the impact of nonlinear distortion, Fig. 7 gives the BER curves and shows a very abnormal phenomenon: due to severe nonlinear distortion, the BER of both 16-QAM and 64-QAM systems increases as the input signal increases.

Each LED chip has an optical power of 0.67 W at the current is 350 mA and we use 16 chips for each TX position. Thus, the optical power of LED L1-L9 is 11 W. We ensure the LED works normally in the linear region by changing the amplitude of the input signal power and then make a performance comparison of OFDM and SC-FDE schemes. Fig. 8 shows the SNR distribution of the 100 different test positions, where the L1-L9 means the location of LEDs.

The performance of 16-QAM modulation system is investigated and compared with 64-QAM modulation in Fig. 9 and the bright color area represents a higher BER value. According to the statistics of the simulation results, the BER performance of OFDM and SC-FDE system with 16-QAM modulation did not show much difference, the BER values below 3.8×10^{-3} (limitation of pre-forward error correction [5]) in the 100 test points of the two systems accounted for 46% and 31%, respectively. For higher modulation orders, such as in 64-QAM

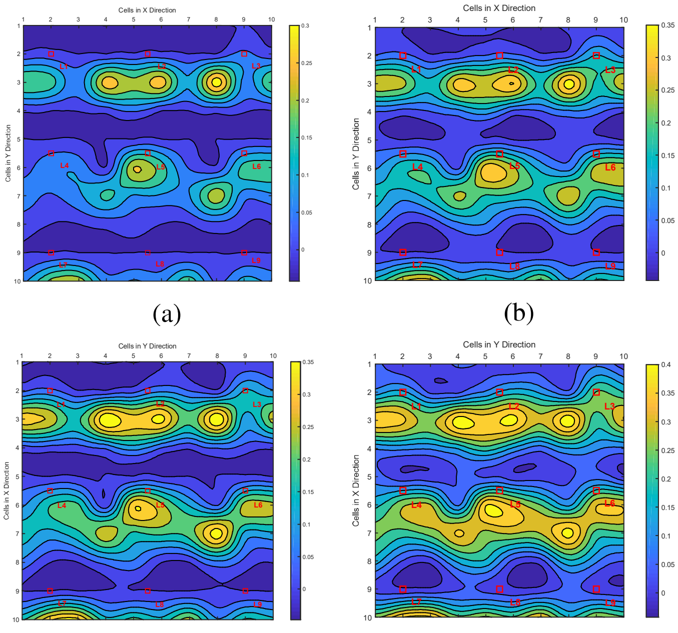

(a) (b) (c) (d)

Fig. 9. The BER comparison of the 100 different test positions between OFDM and SC-FDE in the indoor empty room scenario. (a) OFDM with 16-QAM modulation. (b) OFDM with 64-QAM modulation. (c) SC-FDE with 16-QAM modulation. (d) SC-FDE with 64-QAM modulation.

systems, there are still 16 test points in OFDM system have a BER value lower than 3.8×10^{-3}, but the minimum value of SC-FDE system has reached 7.6×10^{-3}. It can also be verified through Fig.9 that decreasing the QAM order improving the BER performance obviously for both the two systems and the overall BER of OFDM system is significantly lower than that of SC-FDE, which can be clearly seen from the color distribution. In addition, we can note that the BER of the system directly below the LED is not optimal absolutely since the light from Tx is blocked by the human head.

IV. Conclusion

VLC system based on OFDM and SC-FDE under a memory nonlinear LED model has been studied and compared in this paper. We analyzed the BER and PAPR performance of these two systems in a simulated VLC channel scenario furtherly. Simulation results indicate that OFDM scheme exhibits a lower BER value than that of SC-FDE schemes under the same experimental condition. In addition, we discussed the impact of LED nonlinear characteristic and verified that the distortion of signal caused by the inherent nonlinearity of LED will deteriorate the system BER severely.

V. Acknowledgment

This work was supported by Shandong Provincial Natural Science Foundation (ZR2017MF012), the National Key R&D Program of China under Grant 2018YFB1801101, Key Research and Development Program of Shandong Province (2018GGX101009 and 2016GGX101014), the National Natural Science Foundation of China (NSFC) under Grant 61960206006, the Frontiers Science Center for Mobile Information Communication and Security, the High Level Innovation and Entrepreneurial Research Team Program in Jiangsu, the High Level Innovation and Entrepreneurial Talent Introduction Program in Jiangsu, the Research Fund of National Mobile Communications Research Laboratory, Southeast University, under Grant 2020B01, the Fundamental Research Funds for the Central Universities under Grant 2242020R30001, the Huawei Cooperation Project, the EU H2020 RISE TESTBED2 project under Grant 872172, and the Taishan Scholar Program of Shandong Province.

References

[1] P. H. Pathak, X. Feng, P. Hu and P. Mohapatra, “Visible Light Communication, Networking, and Sensing: A Survey, Potential and Challenges,” *IEEE Commun. Surv. Tutor.*, vol. 17, no. 4, pp. 2047–2077, Fourthquarter 2015.

[2] K. Langer, J. Vucic, C. Kottke, L. F. del Rosal, S. Nerreter and J. Walewski, “Advances and prospects in high-speed information broadcast using phosphorescent white-light LEDs,” in *2009 11th International Conference on Transparent Optical Networks*, Azores, 2009, pp. 1–6.

[3] K. Ying, Z. Yu, R. J. Baxley, H. Qian, G. Chang and G. T. Zhou, “Nonlinear distortion mitigation in visible light communications,” *IEEE Wirel Commun*, vol. 22, no. 2, pp. 36–45, April 2015.

[4] H. Li, X. Chen, B. Huang, D. Tang and H. Chen, “High Bandwidth Visible Light Communications Based on a Post-Equalization Circuit,” *IEEE Photon. Technol. Lett*, vol. 26, no. 2, pp. 119–122, Jan.15, 2014.

[5] X. Huang, J. Shi, J. Li, Y. Wang and N. Chi, “A Gb/s VLC Transmission Using Hardware Preequalization Circuit,” *IEEE Photon. Technol. Lett*, vol. 27, no. 18, pp. 1915–1918, 15 Sept.15, 2015.

[6] B. Inan, S. C. Jeffrey Lee, S. Randel, I. Neokosmidis, A. M. J. Koonen and J. W. Walewski, “Impact of LED Nonlinearity on Discrete Multitone Modulation,” *IEEE/OSA J. Optical Commun. and Networking*, vol. 1, no. 5, pp. 439–451, Oct. 2009.

[7] X. Deng et al., “Mitigating LED Nonlinearity to Enhance Visible Light Communications,” *IEEE Trans. Commun.*, vol. 66, no. 11, pp. 5593–5607, Nov. 2018, doi: 10.1109/TCOMM.2018.2858239.

[8] A. Y. Kibangou and G. Favier, “Wiener-Hammerstein systems modeling using diagonal Volterra kernels coefficients,” *IEEE Sig. Proc. Lett.*, vol. 13, no. 6, pp. 381–384, June 2006.

[9] M. Afgani, H. Haas, H. Elgala, and D. Knipp, Visible light communication using OFDM, in *Proc. 2nd Int. Conf. TRIDENTCOM*, 2006, pp. 129 pp.C-134.

[10] J. Armstrong, OFDM for optical communications, *J. Lightwave. and Technol*, vol. 27, no. 3, pp.189–204, 2009

[11] P. Fahamuel, J. Thompson and H. Haas, “Study, analysis and application of optical OFDM, single carrier (SC) and MIMO in intensity modulation direct detection (IM/DD),” in *IET Intelligent Signal Processing Conference 2013 (ISP 2013)*, London, 2013, pp. 1–6.

[12] S. D. Dissanayake and J. Armstrong, “Comparison of ACO-OFDM, DCO-OFDM and ADO-OFDM in IM/DD Systems,” *J. Lightwave. and Technol*, vol. 31, no. 7, pp. 1063–1072, April1, 2013.

[13] R. Touhami, D. Slimani and A. Khelil, “Analysis of an OFDM based Indoor Visible Light Communication System,” in *2018 International Conference on Communications and Electrical Engineering (ICCEE)*, El Oued, Algeria, 2018, pp. 1–4.

[14] D. Falconer, S. L. Ariyavisitakul, A. Benyamin-Seeyar and B. Eidson, “Frequency domain equalization for single-carrier broadband wireless systems,” *IEEE Commun Mag*, vol. 40, no. 4, pp. 58–66, April 2002.

[15] Y. Celik, R. C. Kizilirmak, N. Odabasioglu and M. Uysal, “On the performance of SC-FDE schemes with decision feedback equalizer for visible light communications,” in *2015 17th International Conference on Transparent Optical Networks (ICTON)*, Budapest, 2015, pp. 1–4.

[16] Doyle, F. J., Pearson, R. K., & Ogunnaike, B. A. (2002). Identification and control using Volterra models (pp. 79-103). London: Springer.

[17] T. Komine and M. Nakagawa, “Fundamental analysis for visible-light communication system using LED lights,” *IEEE Trans. Consum. Electron.*, vol. 50, no. 1, pp. 100–107, Feb. 2004.

[18] Uysal, M. Miramirkhani, F. Baykas, T. and Qaraqe, K. IEEE 802.11 bb reference channel models for indoor environments. 2018.